Hindawi
Shock and Vibration
Volume 2021, Article ID 3869045, 11 pages
https://doi.org/10.1155/2021/3869045

Research Article

Experimental and Numerical Study of Strength and Failure Behavior of Precracked Marble under True Triaxial Compression

Yong Han,[1] **Yuemao Zhao**,[2] **and Jinglong Li**[3]

[1]*School of Qilu Transportation, Shandong University, Jinan 250002, Shandong, China*
[2]*College of Energy and Mining Engineering, Shandong University of Science and Technology, Qingdao 266590, Shandong, China*
[3]*School of Civil Engineering, Shandong University, Jinan 250002, Shandong, China*

Correspondence should be addressed to Jinglong Li; 215549020@qq.com

Received 14 October 2021; Accepted 19 November 2021; Published 30 December 2021

Academic Editor: Xing-Dong Zhao

Cracks play an important role in evaluating the strength and failure behavior of engineering rock mass. In order to increase the understanding of strength and failure mechanism of precracked rock, crack propagation and coalescence from preexisting cracks under true triaxial compression are investigated using true triaxial compression tests and Cellular Automata Software for engineering Rockmass fracturing process (CASRock). Three types of specimens were studied experimentally and numerically. Experimental and numerical results show that both the preferential angle and areal intensity of preexisting cracks can affect the compressive strength and failure behavior of the specimens. The peak strength firstly decreases and then increases with increase of the preferential angle. Also, the peak strength nonlinearly decreases with the increase of cracks' areal intensity. The numerical results show that the crack initiation and coalescence are observed and characterized from the inner and outer tips of preexisting cracks in specimens containing single crack and multiple parallel cracks. The main shear failure in the specimen containing multiple unparallel preexisting cracks initiate and propagate from one of the macroscopic preexisting cracks, and other preexisting cracks do not initiate, propagate, and coalesce until reaching the peak strength.

1. Introduction

Rock mass is a complex combination of multiphase materials, which usually contains many joints, cracks, and other defects. These defects greatly reduce the integrity and continuity of rock mass, resulting in changes in mechanical properties and failure mechanism [1–3]. In the construction of tunnel and mine, excavation will cause stress concentration and rotation in the surrounding rock. When the force is loaded on rock mass, preexisting cracks and discontinuities would open and propagate, and new cracks will start to grow at or near the tips of preexisting cracks, even coalescing with preexisting cracks, which would lead to rock mass instability and engineering disasters, such as large deformation and collapse.

With the progress of theory and technology, many scholars have carried out the research on the mechanical properties and failure mechanism of cracked rock using laboratory tests and numerical simulation and have gained some research achievements.

In laboratory test research, many scholars initially used rock-like materials (glass, gypsum, cement mortar, and so on) and prefabricated one or more cracks on the specimens to conduct uniaxial compression and biaxial compression tests in order to study the influence of cracks on the failure mode and mechanical properties of materials [4–6]. Bobet and Einstein [4] studied the fracture coalescence behavior by loading prefractured specimens of gypsum under uniaxial and biaxial compression, and law slippage, wing crack initiation, secondary crack initiation, and crack coalescence were observed. Wong et al. [5] investigated experimentally the peak strength and the mechanisms of crack coalescence of rock-like materials containing three parallel frictional cracks.

Although the influence of cracks on the mechanical properties and failure mechanism of materials has been well

illustrated by the results rock-like materials, the composition and structure are different from those of real rock materials. Therefore, many scholars use precracked rocks (marble, granite, sand stone, and so on) with good homogeneity to study the mechanical properties of cracked rocks. Lee and Jeon [7] used three materials to understand the characteristics of cracking and crack coalescence, and the results can be used to analyze the stability of rock structures. Li et al. [8] explored the propagation and coalescence of preexisting cracks in marble specimens under uniaxial compressive, and two types of newborn cracks were observed: wing cracks and secondary cracks. Yang et al. [9] analyzed the effect of the coplanar crack angle on mechanical parameters of sandstone containing two coplanar oval cracks and constructed the relation between ligament angle and mechanical parameters. Zhou et al. [10] used the DIC technique to measure fracture characteristics on specimen surface and investigated the coalescence behavior around rectangular cavities in rock under uniaxial compressive. Huang et al. [2] found that the arrangement of the flaws pair would have greater impact on the rock strength, deformation, and crack coalescence pattern than the confining pressure through the conventional triaxial compression tests on sandstone with two preexisting closed cracks.

These laboratory results have enhanced our understanding of the strength and failure modes within precracked rocks under uniaxial, biaxial, and triaxial compression. However, it is difficult to observe the detailed process of crack propagation and coalescence due to the opacity of rock, sealing in the test process, and the rapid development of failure. Therefore, many numerical methods have been developed to simulate crack initiation and propagation under loading. These numerical methods include the discrete element method [11], boundary element method [12, 13], and displacement discontinuity method [5]. In recent decades, a numerical simulation code, the cellular automaton (CA) method [14–18], with local consideration and parallel characteristics has been proposed to simulate the failure processes of rock materials under the uniaxial and polyaxial compression condition. Cellular Automata Software for engineering Rockmass fracturing processes (CASRock) was developed, which can commendably simulate the failure process of heterogeneous rocks and the fracturing process of engineering rock mass [19].

Work in the past mainly focused on propagation and coalescence of single or parallel cracks under uniaxial and biaxial compression, but few researches studied the coalescence of unparallel cracks under true triaxial compression. In fact, cracks in rock are often unparallel or intersecting. In this study, experimental simulation and numerical simulation were adopted to investigate the effects of cracks on compressive strength and failure mode of marble specimens under true triaxial compression. Firstly, true triaxial compression tests were conducted with precracked marble specimens to investigate the effects of cracks on strength and failure behavior. Then, CASRock was used to simulate the specimen containing cracks, aimed at revealing the evolution process of crack initiation, propagation, and coalescence under true triaxial compression.

2. Experimental Study of Mechanical Properties of Precracked Marble under True Triaxial Compression

2.1. A Method Analyzing the Natural Cracks' Geometric Characteristics. In order to better explore the effect of natural cracks on rock mechanical properties, the true triaxial compression tests were conducted by marble containing natural cracks in this study. It is important to measure the cracks' geometric characteristics of natural rock, which is the foundation for the study of rock mechanical properties. The statistical dimension of cracks that were observed was 10–100 mm in length and 0.01–1 mm in width [20]. Zhong et al. [21] established an analysis method of natural crack geometric characteristics by two-dimensional plane sketch in the lateral face of rock specimens and considered the comprehensive influence of crack length and dip angle on mechanical properties of rock under conventional compression tests. Gao et al. [22] investigated the crack effect on rock peak strength and found the peak strength shows a U-shaped variation characteristic trend with increasing of dip angle. Wang et al. [23] studied the effect of crack geometric characteristics on the failure mode and strength of composite rock mass, and the uniaxial compression simulation test of composite rock sample with single fracture was carried out. The results showed that the strength of the composite rock sample had a linear negative correlation with the fracture length and the fracture dip. Liu et al. [24] investigated the mechanical behaviors of specimens containing combined flaws with various inclination angles, and the crack initiation, propagation process, and its corresponding mechanisms were studied.

Based on the previous studies [21–28], the intensity and the preferential angle of cracks have important effects on rock mechanical properties. Therefore, these two parameters are calculated by the following method in this paper, as shown in Figure 1.

The length and dip angle in each face of marble specimens are counted by the super-depth-of-field three-dimensional optical microscope. The areal intensity (D_L) is defined as the crack length divided by the specimen area, as shown in the following equation:

$$D_L = \frac{\sum_{i=1}^{N} L_i}{S}, \tag{1}$$

where L_i is the length of crack, N is the total number of cracks in lateral face of specimen, and S is the area of lateral face of the specimen. Based on the typical failure modes under true triaxial tests [29], it is found that the final fracture plane is parallel to the direction of the intermediate principal stress (σ_2) due to the constraint of the intermediate principal stress on the crack opening in the σ_2 direction [29, 30]. Considering that the final fracture plane after test is parallel to the direction of the intermediate principal stress, in this study, a couple of lateral faces of marble specimen where the total areal intensity is larger than the other two lateral faces are placed on the intermediate principal stress loading plane

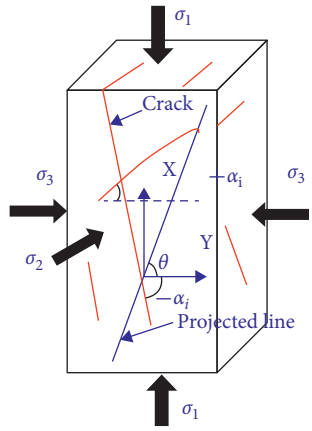

Figure 1: Schematic view of statistical method for evaluating the natural cracks' geometric characteristics of rock specimens.

in order to better explore the effect of natural cracks on the rock mechanical properties.

Then, the total length of all cracks in the intermediate principal stress loading plane is projected in a certain direction, as shown in Figure 1, and the total length of the all cracks projected in this direction is calculated:

$$L_\theta = \sum_{i=1}^{N} l_i \cos(\theta_k - \alpha_i), \tag{2}$$

where α_i is the dip angle of the crack I, θ_k is the preselected angle between projected line and the σ_1 loading plane, and the range of θ_k is -90°~$+90^\circ$. The increment of θ_k in this paper is 5, and the maximum of k is 36.

According to determination method of the preferential angle of cracks [21, 22], the angle with the maximum projection length is the preferential angle of cracks:

$$\theta_p = \{\theta_k \mid \mathrm{Max}[L_\theta(\theta_k, \alpha_i, l_i)]\}. \tag{3}$$

The areal intensity (D_L) and the preferential angle (θ_p) are used to analyze the effect of crack geometric characteristics on the mechanical properties of marble.

2.2. Specimens and Testing Apparatus. The marble used for tests came from Jinchuan nickel mine, located in Jinchuan, Gansu Province, China. Rectangular prismatic specimens of marble, $50 \times 50 \times 100$ mm in size, were prepared for true triaxial compression tests. The experimental investigation of specimens was accomplished considering the three cases: (a) intact specimens, (b) specimens containing a single crack, and (c) specimens containing multiple cracks, as shown in Figure 2. The density of specimens is about 2.75 g/cm^3. The tests were conducted on the novel Mogi type of the true triaxial testing system (Lavender 508) of Northeast University developed by Feng et al. [31]. The tests were carried out at a stress level of $\sigma_2 = 50$ MPa and $\sigma_3 = 30$ MPa.

2.3. Experimental Results. The experimental results show that the peak strength of marble containing single natural crack (D_L is kept around 0.00953–0.01038 m^{-1}) firstly decreases and then increases with increase of the preferential angle, as shown in Figure 3. The peak compressive strength is 361 MPa at $\theta_p = 3^\circ$, which is close to the compressive strength of intact marble. The peak compressive strength is 285 MPa at $\theta_p = 75^\circ$. Compared with the compressive strength of intact marble at the same stress level, it is reduced by 86 MPa.

Figure 4 shows that peak strength nonlinearly decreases with the increase of cracks' areal intensity, when θ_p is kept at 65°. When the areal intensity is 0.0457 m^{-1}, the tested specimen has a compressive strength of about 258 MPa. It is reduced by 113 MPa, compared with the compressive strength of intact marble at the same stress level. Therefore, it can be seen from the experimental results that the cracks' geometric characteristics have a great influence on the mechanical properties of marble.

3. Numerical Study of Mechanical Properties of Precracked Marble under True Triaxial Compression

Based on the experimental study of intact and precracked marble specimens, the effect of cracks' geometric characteristics on the strength of marble has been obtained. However, it is difficult to observe the detailed process of rock fracture and crack propagation. Therefore, a numerical simulation using Cellular Automata Software for engineering Rockmass fracturing processes (CASRock) was carried out for the precracked marble specimens.

3.1. Descriptions of Cellular Automata Software for Engineering Rockmass Fracturing Processes (CASRock). Cellular Automata Software for engineering Rockmass fracturing processes (CASRock) was developed to solve the problem of the fracturing process for engineering rock mass, which is a combination of cellular automaton, rock mechanics, engineering geology, elastoplastic mechanics, and fracture mechanics [16]. The process is a "down-top" way of handling the fracturing behavior of rock mass. A cellular automaton is mainly composed of cell, cell space, cell state, neighborhood, and updating rule [16–18]. The rock mass to be simulated is put into a system composed of cells. Figure 5 shows the relationship between cell and its neighbors in the development of updating rule [17]. The purpose of this paper is to study the failure process of cracked marble under true triaxial compression, so all the components should be defined in a three-dimensional domain.

In order to model the precracked specimens, a rock discontinuous cellular automaton [18] was developed. Its updating rule is more complex because there are internal boundaries, as shown in Figure 6 [18].

The cell is the basic component of the cellular automaton [15], and it can be defined as

(a) (b) (c)

Figure 2: View of the specimens: (a) intact specimen, (b) specimen containing a single crack, and (c) specimen containing multiple cracks.

$$D_i = N_i \cup \left\{E_i^1, \ldots, E_i^{m_i}; N_i^1, \ldots, N_i^{n_i}, N_i \in E_i^j \mid N_i^k \in E_i^j, \quad j = 1, \ldots m_i\right\}, \tag{4}$$

where D_i is the cell, which is composed of cell nodes N_i, corresponding to cell elements E_i^j, and neighboring cell nodes N_i^k.

In the cellular automaton model, the equilibrium equation [15, 17, 18] of each cell can be defined as follows:

$$K_{ij}\Delta u_j = \Delta F_i, \tag{5}$$

where K_{ij} is the local stiffness on the cell node, Δu_j is the incremental degree of freedom, and ΔF_i is the nodal force. The dimension of K_{ij}, Δu_j, and ΔF_i is dependent on the cell type.

The increment nodal force ΔF_i^k on the neighboring cells [17] is calculated by the following equation:

$$\left\{\Delta F_i^k\right\} = \left[B_{im}^j\right]\left\{\Delta u_m\right\}, \tag{6}$$

where B_i^j is the cell element stiffness.

In CASRock, each cell follows updating rule described in equations (5) and (6), and the system can get static equilibrium state when the self-organization phenomenon of $\Delta u_i \longrightarrow 0$ or $\Delta F_i \longrightarrow 0$ is reached [15, 17, 18].

In this paper, the 3D elastic-plastic-ductile-brittle mode [32] is selected to describe the response of marble materials. This model considers the asymmetric effect of intermediate principal stress on the strength of hard rock, and it can be more consistent with true triaxial compression. The failure function can be expressed as [32]

$$\begin{aligned} F &= \left(\frac{\sigma_1 - \sigma_3}{\sin\varphi_b}\right)^2 - \left(\sigma_1 + \sigma_3 + 2c_0\cot\varphi_0\right)^2 + \left(2\sigma_t + 2c_0\cot\varphi_0\right)^2, \\ \sin\varphi_b &= \frac{\sin\varphi_0}{\sqrt{1 - b + sb^2} + t\left(1 - \sqrt{1 - b + sb^2}\right)\sin\varphi_0}, \end{aligned} \tag{7}$$

where b is intermediate principal stress coefficient, which can be expressed as

$$b = \frac{\sigma_2 - \sigma_3}{\sigma_1 - \sigma_3}, \tag{8}$$

where c_0, φ_0, and σ_t are the cohesion, friction angle, and uniaxial tension strength, respectively, s is the strength-difference coefficient between generalized triaxial extension and generalized triaxial compression, and t is the material constant controlling the maximum strength-increasing ratio affected by σ_2.

3.2. Numerical Simulation Schemes. Figure 7 shows the setup of the numerical models. In the numerical model, the size of the specimens is designed to match the specimens in the experimental tests. As for the single crack and parallel cracks, the length is 50 mm, and the distance between two cracks is 5 mm, respectively. The parameters of the specimens for numerical simulations are shown in Table 1. In this paper, two cases are stimulated. In Case 1, in order to study the effect of different preferential angles and areal intensity on the strength and failure modes of the specimens, three

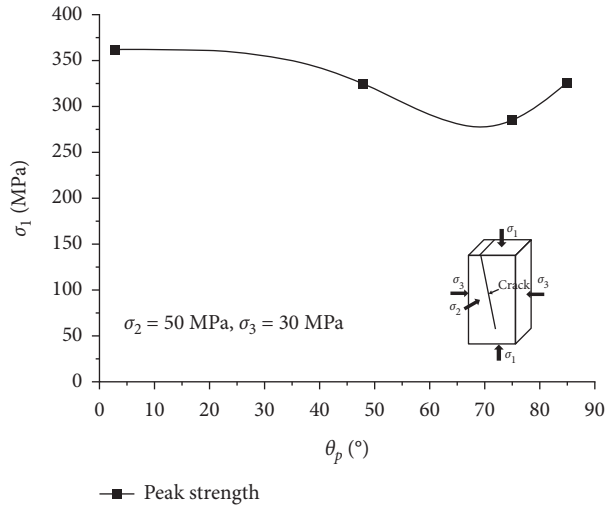

Figure 3: Experimental results of the preferential angle (θ_p) effect on the peak stress of marble containing single crack.

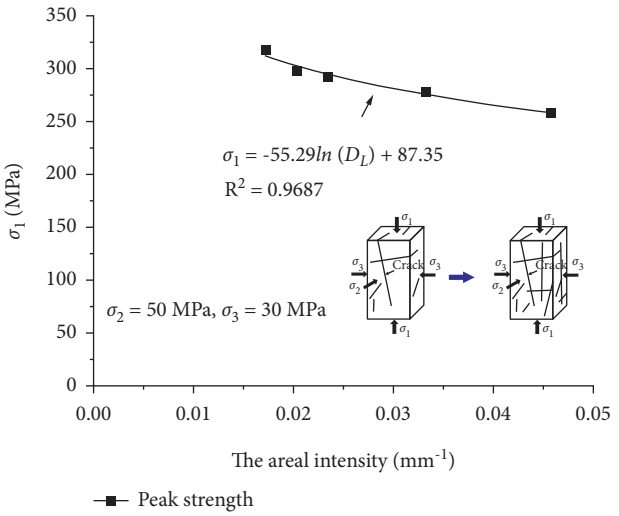

Figure 4: Experimental results of the areal intensity (D_L) effect on the peak stress of marble containing multiple cracks.

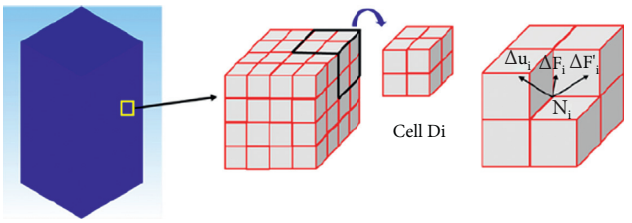

Figure 5: Numerical model and three-dimensional domain to be solved.

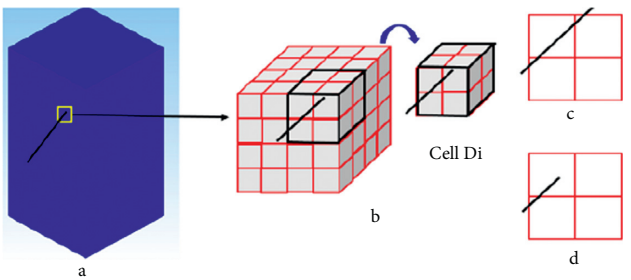

Figure 6: Representation of the discontinuous cellular automaton model and its different states.

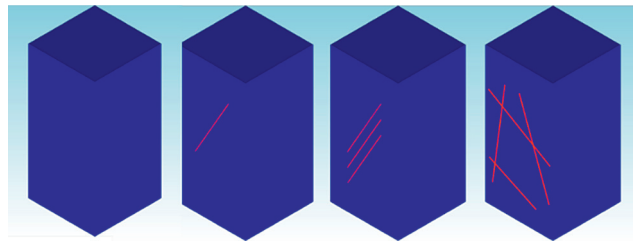

Figure 7: Numerical model of intact and precracked specimens: (a) intact specimen, (b) specimen containing single crack, (c) specimen containing multiple parallel cracks, and (d) specimen containing multiple unparallel cracks.

Table 1: Parameters used in CASRock.

Parameters	Marble	Crack	Parameters	Marble	Crack
Young's modulus (GPa)	80	60	Poisson's ratio	0.35	0.35
Initial cohesion (MPa)	15	5	Residual cohesion (MPa)	3	3
Initial friction angle (°)	50.8	40	Residual frictional angle (°)	45	45
Homogeneous index (m)	8	8	Seed parameter (s)	10	10

types of crack geometry characteristics are considered. Type A is the case of intact marble without cracks, and Type B and Type C are specimens containing single crack and multiple parallel cracks with different preferential angles. In Case 2, in order to analyze the process of unparallel crack coalescence, Type D containing multiple unparallel cracks is established, which is set up based on the geometric characteristics of natural cracks in test specimens. A detailed description of these specimens with different crack geometric characteristics is presented in Table 2. The numerical simulation was carried out at a stress level of $\sigma_2 = 50$ MPa and $\sigma_3 = 30$ MPa.

3.3. Simulation Results

3.3.1. Effects of the Preferential Angle on the Strength and Failure Modes. Figure 8 shows the complete stress-strain curves of specimens containing single crack with different preferential angles, when D_L is kept at 0.01 m^{-1}. The variation trend of strength with preferential angle obtained from simulation is similar to the experimental results. The peak strength of specimens containing single crack firstly decreases and then increases with the increase of the preferential angle (Figure 9).

Figure 10 compares the crack evolutions of intact and cracked specimens obtained from numerical results. In the intact specimen, the microdamage initiates at the surface of the marble specimen, and the failure mode is shear failure. When specimens contain single crack, failure modes under true triaxial compression include two modes. In mode 1, the failure mode of specimen is main shear failure, when the preferential angle is close to 0° or 90°, which was same as the intact marble, but there are other macrocracks instead of one within intact marble, as shown in Figure 10(a). The microdamage initiated mainly from the tips of the preexisting crack and the surface of the specimens. The shear failure is caused by the crack initiation and coalescence at the surface of the specimens. The preexisting crack initiation results in tensile failure. In mode 2, the failure mode of the specimen partly coincides with the plane of the crack or occurs totally along the preexisting crack. Also, the failure angle is same as the preferential angle (60°). Figure 11 shows the final failure mode comparison between the experimental and numerical simulation results. It can be found that the simulation results are consistent with the experimental results. Therefore, this method can be used to study the failure evolution process of precracked specimens under true triaxial compression.

3.3.2. Effects of the Areal Intensity on the Strength and Failure Modes. Figure 12 shows the complete stress-strain curves of specimens containing multiple parallel cracks, when the preferential angle is kept at 45°. With the increase of the areal intensity, the peak strength of specimens decreases nonlinearly, as shown in Figure 13.

Figure 14 shows the numerically simulated microdamage evolutions from the macroscopic preexisting cracks with different areal intensities. When the specimens contain multiple parallel cracks, microdamage initiates from the tips of the one or two preexisting cracks and propagates gradually along the preexisting cracks. Then, some shear cracks grow and coalesce. Then, the final macrofailure mode is shear failure, which is caused by preexisting crack coalescence.

3.3.3. Analysis of Cracks' Coalescence in Specimens Containing Unparallel Cracks. In the underground engineering construction, the fracture distribution state is extremely complex, including parallel and cross distribution. In order to better reveal the failure evolution process of cracked rock mass, this paper establishes a model of marble specimen containing intersected cracks to explore the evolution process of crack initiation, propagation, and coalescence under true triaxial compression.

Table 2: Crack geometries of precracked specimens.

Type	The preferential angles (°)	The areal intensity (m^{-1})	Type	The preferential angles (°)	The areal intensity (m^{-1})
A	Intact marble (no crack)		B	90	0.010
	0	0.010		45	0.020
	30	0.010	C	45	0.030
B	45	0.010		45	0.040
	60	0.010		45	0.050
	75	0.010	D	65	0.045

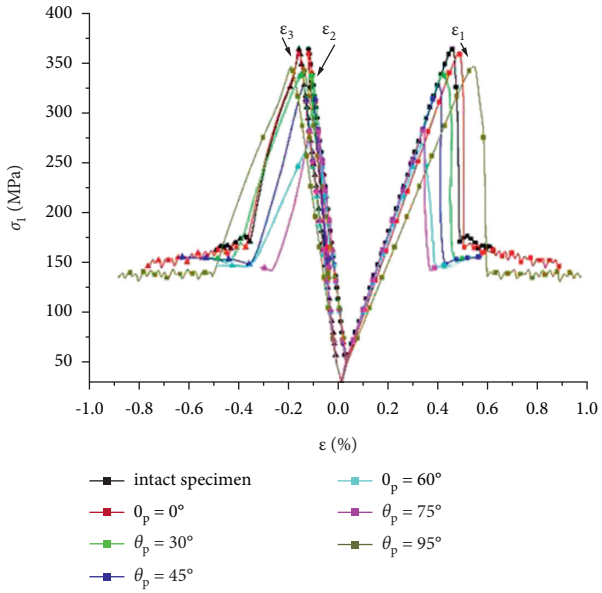

Figure 8: The stress-strain curves of specimens containing single crack with different preferential angles.

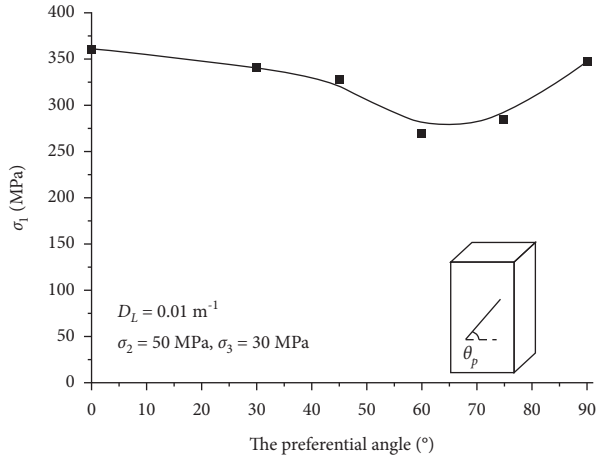

Figure 9: Effect of preferential angle on the strength of specimens containing single crack.

Figure 15 shows the numerical and experimental failure modes of specimens containing intersected cracks. It can be seen that the numerical failure mode has a good agreement with the experimental results in terms of coalescence characteristics. As indicated previously, it is difficult to observe the microdamage evolutions in laboratory testing.

Figure 16 shows the crack evolutions during the loading process. During the elastic deformation stage, there is no obvious damage region. At the first peak value, the main shear cracks initiate and propagate from one of the macroscopic preexisting cracks. Due to the penetration of crack, the peak strength drops slowly with increase of ε_1. It can be explained that this failure is caused by the penetration of preexisting cracks, and other researchers also obtained similar results by experimental and numerical study [2, 7]. Subsequently, the failure of specimens develops along the

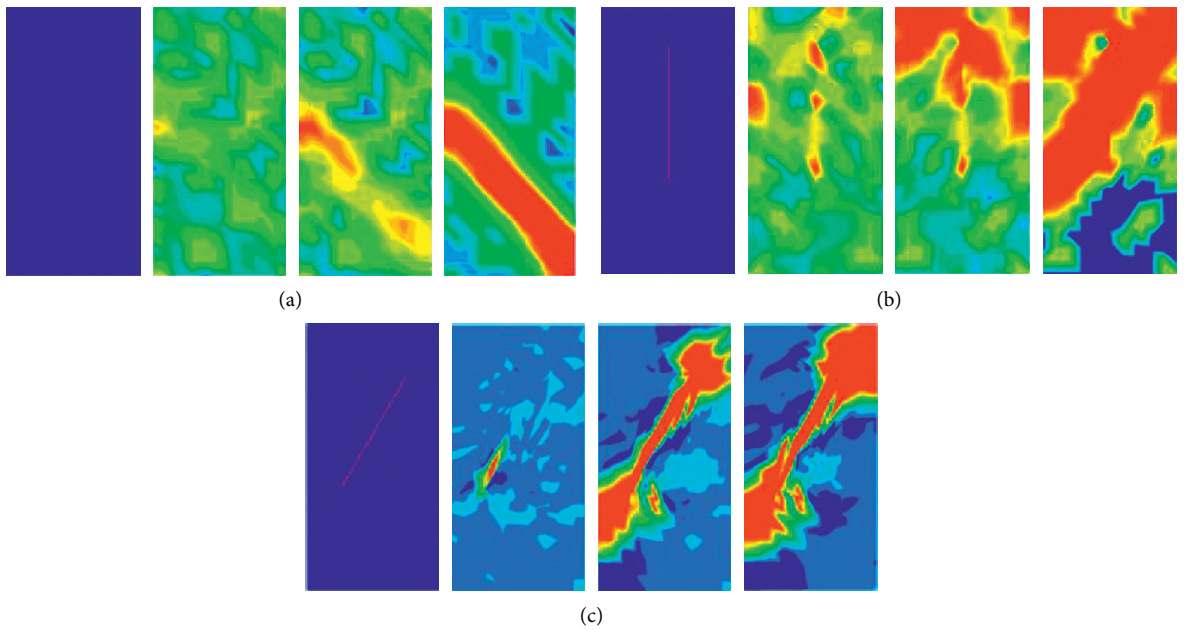

Figure 10: Numerically simulated crack evolution in specimens containing single crack with different preferential angles. (a) Intact specimens. (b) $\theta_p = 90^\circ$. (c) $\theta_p = 60^\circ$.

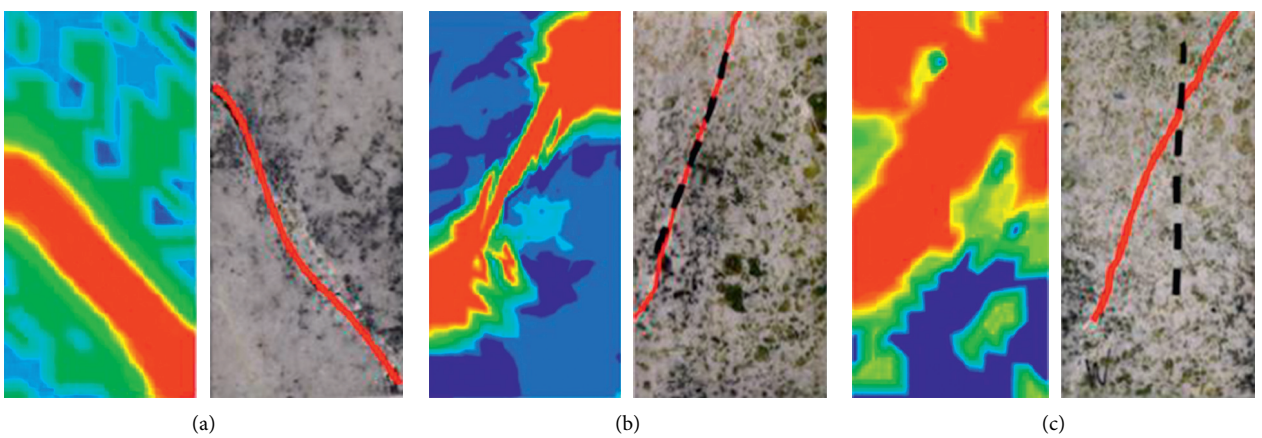

Figure 11: Comparison of experimental results and numerical simulation results.

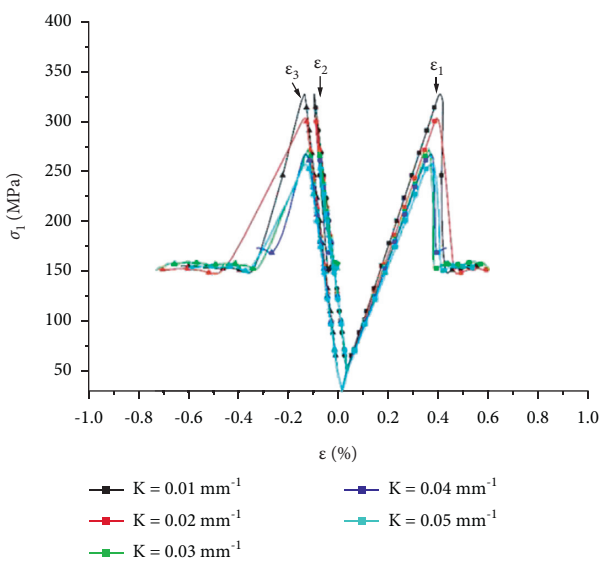

Figure 12: The stress-strain curves of specimens containing multiple parallel cracks.

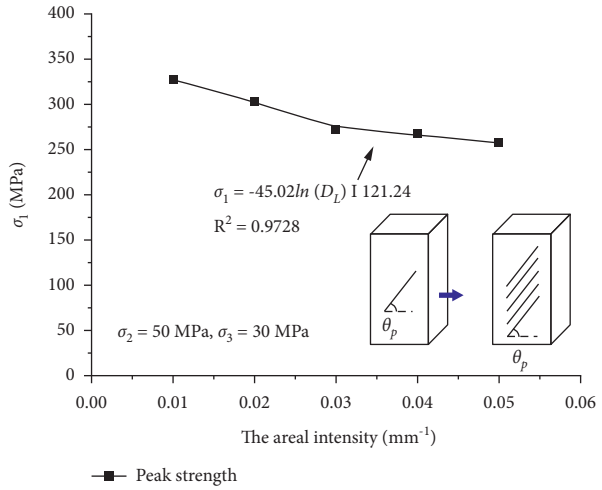

Figure 13: Effect of the areal intensity on the strength of specimens containing multiple parallel cracks.

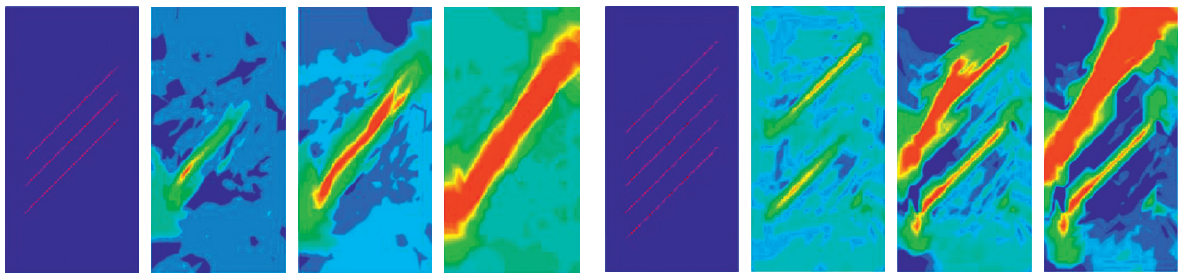

Figure 14: Numerically simulated crack evolution in specimens containing multiple parallel cracks.

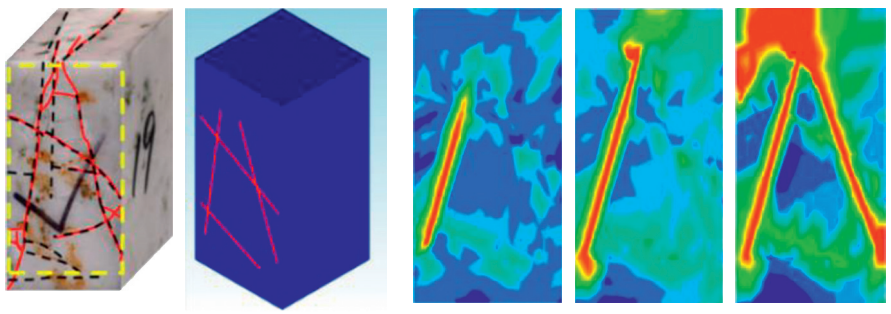

Figure 15: (a) The numerical and experimental failure modes of specimens and (b) crack evolution in specimens containing multiple parallel cracks.

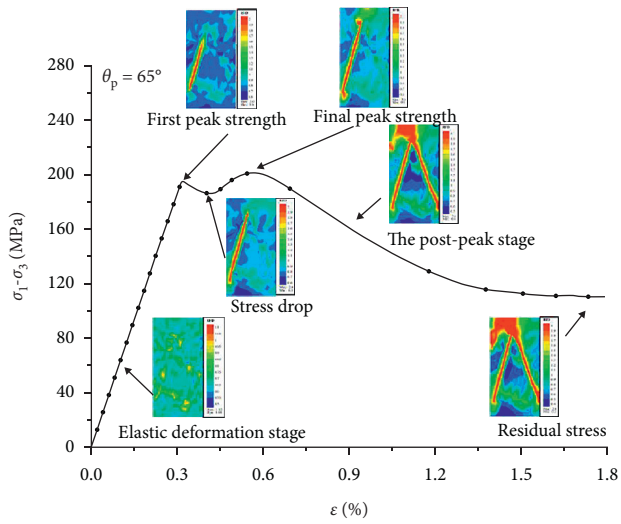

Figure 16: Crack initiation and coalescence process during the process of true triaxial compression.

preexisting crack and spreads to the intact rock part before the stress level reaches the second peak stress. Entering the postpeak stage, the other preexisting cracks also initiate, propagate, and coalesce to form a macrofailure until reaching the residual strength.

4. Conclusions

In this study, firstly, a series of true triaxial compression tests and numerical simulations using CASRock were conducted on intact marble and precracked marble specimens. Based on the results, the effects of cracks' geometric characteristics on strength and failure modes were analyzed, and the following conclusions are drawn:

(1) With the increase of the preferential angle, the peak strength firstly decreases and then increases. Also, the peak strength nonlinearly decreases with the increase of cracks' areal intensity.

(2) The crack initiation and coalescence are observed and characterized from the inner and outer tips of preexisting cracks in specimens containing single crack and multiple parallel cracks.

(3) The failure mode of the specimen is main shear failure, when the preferential angle is close to 0° or 90°. The failure mode of the specimen partly coincides with the plane of the crack or occurs totally along the preexisting crack, when the preexisting crack dip angle is close to the failure angle of the intact specimen.

(4) For the specimens containing multiple unparallel cracks, the main shear failure initiate and propagate from one of the macroscopic preexisting cracks, and other preexisting cracks do not initiate, propagate, and coalesce until reaching the peak strength.

Data Availability

Some or all data, models, and codes generated or used during the study are available from the corresponding author upon request.

Disclosure

The tests in this paper were conducted on a Lavender 508 true triaxial apparatus at Key Laboratory of Ministry of Education on Safe Mining of Deep Metal Mines, Northeastern University, Shenyang, China.

Conflicts of Interest

The authors declare that they have no conflicts of interest.

Acknowledgments

The authors would like to express their gratitude to all members of Key Laboratory of Ministry of Education on Safe Mining of Deep Metal Mines, Northeastern University, Shenyang, China.

References

[1] Y. L. Zhao, L. Y. Zhang, W. J. Wang, C. Pu, W. Wan, and J. Tang, "Cracking and Stress–Strain Behavior of Rock-Like Material Containing Two Flaws Under Uniaxial Compression," *Rock Mechanics and Rock Engineering*, vol. 49, no. 7, pp. 2665–2687, 2016.

[2] D. Huang, D. Gu, C. Yang, R. Huang, and G. Fu, "Investigation on mechanical behaviors of sandstone with two preexisting flaws under triaxial compression," *Rock Mechanics and Rock Engineering*, vol. 49, no. 2, pp. 375–399, 2016.

[3] S. Miao, P.-Z. Pan, Z. Wu, S. Li, and S. Zhao, "Fracture analysis of sandstone with a single filled flaw under uniaxial

compression," *Engineering Fracture Mechanics*, vol. 204, pp. 319–343, 2018.

[4] A. Bobet and H. H. Einstein, "Fracture coalescence in rock-type materials under uniaxial and biaxial compression," *International Journal of Rock Mechanics and Mining Sciences*, vol. 35, no. 7, pp. 863–888, 1998.

[5] R. H. C. Wong, K. T. Chau, C. A. Tang, and P. Lin, "Analysis of crack coalescence in rock-like materials containing three flaws-Part I: experimental approach," *International Journal of Rock Mechanics and Mining Sciences*, vol. 38, no. 7, pp. 909–924, 2001.

[6] M. Sagong and A. Bobet, "Coalescence of multiple flaws in a rock-model material in uniaxial compression," *International Journal of Rock Mechanics and Mining Sciences*, vol. 39, no. 2, pp. 229–241, 2002.

[7] H. Lee and S. Jeon, "An experimental and numerical study of fracture coalescence in pre-cracked specimens under uniaxial compression," *International Journal of Solids and Structures*, vol. 48, no. 6, pp. 979–999, 2011.

[8] Y.-P. Li, L.-Z. Chen, and Y.-H. Wang, "Experimental research on pre-cracked marble under compression," *International Journal of Solids and Structures*, vol. 42, no. 9-10, pp. 2505–2516, 2005.

[9] S.-Q. Yang, Y.-H. Huang, W.-L. Tian, and J.-B. Zhu, "An experimental investigation on strength, deformation and crack evolution behavior of sandstone containing two oval flaws under uniaxial compression," *Engineering Geology*, vol. 217, pp. 35–48, 2017.

[10] Z. Zhou, L. Tan, W. Cao, Z. Zhou, and X. Cai, "Fracture Evolution and Failure Behaviour of marble Specimens Containing Rectangular Cavities under Uniaxial Loading," *Engineering Fracture Mechanics*, vol. 184, 2017.

[11] L. F. Vesga, L. E. Vallejo, and S. Lobo-Guerrero, "DEM analysis of the crack propagation in brittle clays under uniaxial compression tests," *International Journal for Numerical and Analytical Methods in Geomechanics*, vol. 32, pp. 1405–1415, 2010.

[12] A. Manouchehrian, M. Sharifzadeh, M. F. Marji, and J. Gholamnejad, "A bonded particle model for analysis of the flaw orientation effect on crack propagation mechanism in brittle materials under compression," *Archives of Civil and Mechanical Engineering*, vol. 14, no. 1, pp. 40–52, 2014.

[13] M. Cai, "Influence of intermediate principal stress on rock fracturing and strength near excavation boundaries-Insight from numerical modeling," *International Journal of Rock Mechanics and Mining Sciences*, vol. 45, no. 5, pp. 763–772, 2008.

[14] A. K. Bandpey, K. Shahriar, M. Sharifzadeh, and P. Marefvand, "Comparison of methods for calculating geometrical characteristics of discontinuities in a cavern of the Rudbar Lorestan power plant,," *Bulletin of Engineering Geology and the Environment*, vol. 78, no. 1, 2017.

[15] X.-T. Feng, P.-Z. Pan, and H. Zhou, "Simulation of the rock microfracturing process under uniaxial compression using an elasto-plastic cellular automaton," *International Journal of Rock Mechanics and Mining Sciences*, vol. 43, no. 7, pp. 1091–1108, 2006.

[16] P.-Z. Pan, X.-T. Feng, and J. A. Hudson, "Study of failure and scale effects in rocks under uniaxial compression using 3D cellular automata," *International Journal of Rock Mechanics and Mining Sciences*, vol. 46, no. 4, pp. 674–685, 2009.

[17] P.-Z. Pan, F. Yan, and X.-T. Feng, "Modeling the cracking process of rocks from continuity to discontinuity using a cellular automaton," *Computers & Geosciences*, vol. 42, pp. 87–99, 2012.

[18] P.-Z. Pan, X.-T. Feng, and J. A. Hudson, "The influence of the intermediate principal stress on rock failure behaviour: a numerical study," *Engineering Geology*, vol. 124, pp. 109–118, 2012.

[19] X. T. Feng, P. Z. Pan, Z. Wang, and Y. Zhang, "Development of cellular automata software for engineering rockmass fracturing processes," in *Challenges and Innovations in Geomechanics. IACMAG 2021*, M. Barla, A. Di Donna, and D. Sterpi, Eds., Springer, New York, NY, USA, 2021.

[20] Y. S. Zhou and L. Zhang, "Statistics and Analysis of Drilling Core Fractures of Fractured Reservoirs," *World Geology*, vol. 19, pp. 117–124, 2000.

[21] Z. S. Zhong, R. G. Deng, Y. Sun, and L. Lu, "Geometric characterization of natural crack network in rhyolite," *Chinese Journal of Rock Mechanics and Engineering*, vol. 36, pp. 167–174, 2017.

[22] Y. Gao, X.-T. Feng, Z. Wang, and X. Zhang, "Strength and failure characteristics of jointed marble under true triaxial compression," *Bulletin of Engineering Geology and the Environment*, vol. 79, no. 2, pp. 891–905, 2019.

[23] Q. H. Wang, J. Wang, and U. C. Ye, "Effect of single fracture geometric characteristics of composite rock samples on its failure mode and strength," *Metal Mine*, vol. 2, pp. 134–140, 2020.

[24] T. Liu, B. Lin, Q. Zou, C. Zhu, and F. Yan, "Mechanical behaviors and failure processes of precracked specimens under uniaxial compression: a perspective from microscopic displacement patterns," *Tectonophysics*, vol. 672-673, pp. 104–120, 2016.

[25] Z. S. Zhong, R. G. Deng, J. Li, and X. M. Fu, "Experimental study of triaxial mechanical properties of naturally fissured rhyolite," *Chinese Journal of Rock Mechanics and Engineering*, vol. 33, p. 1233, 2014.

[26] P. Hamdi, D. Stead, and D. Elmo, "Characterizing the influence of stress-induced microcracks on the laboratory strength and fracture development in brittle rocks using a finite-discrete element method-micro discrete fracture network FDEM-μDFN approach," *Journal of Rock Mechanics and Geotechnical Engineering*, vol. 7, no. 6, pp. 609–625, 2015.

[27] D. E. Moore and D. A. Lockner, "The role of microcracking in shear-fracture propagation in granite," *Journal of Structural Geology*, vol. 17, no. 1, pp. 95–111, 113-114, 1995.

[28] C. Z. Pu, P. Cao, and L. Y. Zhang, "Numerical analysis and strength experiment of rock-like materials with multi-fissures under uniaxial compression," *Rock and Soil Mechanics*, vol. 31, pp. 3661–3666, 2010.

[29] X.-T. Feng, B. Haimson, X. Li et al., "ISRM suggested method: determining deformation and failure characteristics of rocks subjected to true triaxial compression," *Rock Mechanics and Rock Engineering*, vol. 52, no. 6, pp. 2011–2020, 2019.

[30] R. Kong, X.-T. Feng, X. Zhang, and C. Yang, "Study on crack initiation and damage stress in sandstone under true triaxial compression," *International Journal of Rock Mechanics and Mining Sciences*, vol. 106, pp. 117–123, 2018.

[31] X.-T. Feng, X. Zhang, R. Kong, and G. Wang, "A novel Mogi type true triaxial testing Apparatus and its use to obtain complete stress-strain curves of hard rocks," *Rock Mechanics and Rock Engineering*, vol. 49, no. 5, pp. 1649–1662, 2016.

[32] X.-T. Feng, R. Kong, C. Yang et al., "A three-dimensional failure criterion for hard rocks under true triaxial compression," *Rock Mechanics and Rock Engineering*, vol. 53, no. 1, pp. 103–111, 2020.